BioMedical Engineering OnLine
https://doi.org/10.1186/s12938-026-01546-1
Article in Press

Experimental quantification of balance using whole-body stability regions from postural sway exercises

Received: 17 Nov 2025
Accepted: 25 Feb 2026
Published online: 07 March 2026

Kübra Akbaş, Neethan Ratnakumar, Rachel Jones, Marianne Doss, Carlotta Mummolo, Jean-François Daneault & Xianlian Zhou

Cite this article as: Akbaş, K., Ratnakumar, N., Jones, R. *et al.* Experimental quantification of balance using whole-body stability regions from postural sway exercises. *BioMed Eng OnLine* (2026). https://doi.org/10.1186/s12938-026-01546-1

Experimental quantification of balance using whole-body stability regions from postural sway exercises

Kübra Akbaş[1], Neethan Ratnakumar[1], Rachel Jones[2], Marianne Doss[3], Carlotta Mummolo[4], Jean-François Daneault[5], Xianlian Zhou[1,*]

1 Department of Biomedical Engineering, New Jersey Institute of Technology, 323 Dr Martin Luther King Jr Blvd, Newark, NJ, USA 07102

2 Department of Biomedical Engineering, Stevens Institute of Technology, Edwin A. Stevens Hall 411, Hoboken, NJ, USA 07030

3 Department of Biological Sciences, New Jersey Institute of Technology, 100 Summit St, Newark, NJ, USA 07102

4 Department of Mechanics, Mathematics, and Management, Politecnico di Bari, Via Orabona 4, Bari, Italy, 70125

5 Department of Rehabilitation and Movement Sciences, Rutgers University School of Health Professions, 65 Bergen St, Newark, NJ, USA 07107

*Corresponding author:

Email: alexzhou@njit.edu (XZ)

ABSTRACT

Background

Comprehensive balance assessment is essential for evaluating balance deficiencies, particularly in individuals with limited mobility and increased fall risk. However, clinical balance assessments often rely on subjective scoring and simplified models that may not capture the full dynamics of human postural control. Additionally, center of pressure (COP)-based metrics and inverted pendulum models offer limited insight into whole-body balance ability. Balance regions (BRs) offer a more holistic approach by quantifying balanced center of mass (COM) states. Previously, BRs were used to assess the balancing capabilities of bipedal systems and humans in simulation; however, there is a lack of real-world implementations of whole-body BR analyses in human balance.

Methods

This study presents a novel experimental framework to quantify human balance using COM-based BRs derived from large postural sway tasks. The participants comprised 22 healthy young adults who performed voluntary, supported, and perturbed anterior–posterior (AP) sway exercises while standing on force plates, with a full-body motion capture setup. COM trajectories were obtained from individualized musculoskeletal models in OpenSim to construct BRs, which were compared with linear inverted pendulum (LIP) limits. Key COM-based metrics included maximum AP margin of stability (MoS), maximum AP velocity, extrapolated COM (XcoM) range, and BR areas. COP measures (root mean square (RMS), range, 95% confidence ellipse area, mean AP velocity) and joint kinematics were also analyzed.

Results

COM trajectories largely stayed within the LIP-based analytical boundaries, with BRs capturing individualized balance envelopes. Significant sex differences were observed in the maximum posterior MoS (p=0.01974), XcoM range metrics (p<0.03924), and BR areas (p<0.045). COP metrics varied significantly across tasks in the RMS, 95% confidence ellipse area, and mean velocity (p<0.02046), and inverse kinematics revealed distinct joint coordination patterns during sway; there was a significant sex difference in the COP range during perturbed backward sway (p=0.03053).

Conclusions

This study presents a novel, COM-based experimental framework for balance assessment that captures whole-body stability regions from dynamic postural tasks. BRs provide a quantitative and individualized measure of balance capacity beyond traditional metrics. This framework has potential for fall risk evaluation, balance training, and integration with wearable or markerless motion capture in clinical and neurorehabilitation settings.

KEYWORDS

Balance, musculoskeletal modeling, motion capture, center of mass, center of pressure, inverse kinematics

BACKGROUND

Human balance and postural control are complex physiological processes demanding the coordination of sensory inputs, neural feedback, cognitive processing, and desired motor outputs (1, 2); these intricate systems are essential for maintaining postural stability and avoiding falls in daily life (3). Therefore, understanding and monitoring human balance is essential to address a wide array of health issues spanning various patient populations, as well as in improving sports performance and rehabilitation in athletes. To this end, balance is a multivariate skill that has primarily been studied by observing the ability to maintain stability under various conditions, including standing posture maintenance (4) or during controlled leaning and recovery tasks (5). Similarly, responses to different types of perturbations can also be evaluated to determine balancing ability and resilience, such as through continuous sinusoidal platform shifts (6), sudden push or pull forces applied to the body, optical flow perturbations, and treadmill-based perturbations through sudden deceleration/accelerations (7).

In clinical settings, several functional balance tests are used to evaluate an individual's static and dynamic balancing ability. The Romberg Test (standing with eyes open and closed) (8) and the Single Leg Stance Test (9) are both basic static tests that allow for quick screening of balance issues in patients, whereas the Berg Balance Scale is a functional balance test that evaluates both static and dynamic balance through 14 tasks (10). The Mini-BESTest focuses on dynamic balance tasks and includes items related to anticipatory postural adjustments and reactive postural control, and is considered one of the most comprehensive balance tests (11). Lastly, the Y-Balance Test and the Star Excursion Test (12) are common tests to measure dynamic balance, while the Timed Up-and-Go Test has also been established as a sensitive measure for identifying fall risk (13). Although these tests are well-established and standardized, they often rely on subjective scoring and may be limited in scope, lacking comprehensive quantitative and objective metrics.

To address these limitations, quantitative and objective measures have been explored in the literature; most commonly, a stabilogram analysis is used to assess balance, which tracks the trajectory of the center of pressure (COP), the point where the ground reaction force (GRF) vector is applied. From the stabilogram, metrics such as the range, velocity, and area of the COP trajectory can provide quantitative indicators of postural stability (14). The Limits of Stability test is another key method of balance assessment that evaluates the maximum distance a person can sway in various directions without losing balance, offering a clear, quantifiable measure of balance control and the ability to maintain stability within a defined boundary (15, 16, 17). In addition to these linear approaches, more complex metrics, such as the Lyapunov exponent, quantify the stability of postural control in response to small perturbations over time, providing deeper insights into the dynamic and nonlinear aspects of balance (6).

In addition to stabilograms and COP-based metrics, the mechanics of standing balance in the anteroposterior (AP) direction are often modeled using a linear inverted pendulum (LIP) model, where the body pivots around the ankle and is treated as a rigid rod with its mass concentrated at the center of mass (COM) (2). Within the LIP-based framework, balance is maintained by the body continuously striving to keep the COM within the base of support (BoS), which is defined as the area of contact between the feet and the ground. From the LIP, the margin of stability (MoS) can be obtained as a key metric in assessing balance control, particularly in dynamic conditions; this margin represents the difference between the extrapolated center of mass (XcoM), a predictive measure that incorporates both the position and velocity of the COM, and the edge of the BoS (18). The MoS is defined as the distance between the XcoM and the BoS, with a negative MoS indicating that the XcoM has moved beyond the BoS. The XcoM trajectory and resulting MoS values ultimately signal the need for corrective actions, such as stepping, to restore balance (18). Utilizing these frameworks centered around the MoS and XcoM concepts offers a robust approach for understanding balance control during dynamic movements and predicting potential balance recovery (18, 19).

While the MoS assesses the immediate state of balance and the potential for corrective actions, more comprehensive methodologies, such as the Balance Region (BR), have been developed to evaluate stability over a range of conditions (20, 21). The BR is a state-space region that defines the set of feasible COM positions and velocities where stability can be maintained without requiring corrective actions, such as stepping. The BR overall encapsulates the dynamics of postural control, accounting for both the position and velocity of the COM. The boundaries of the BR (i.e., BR envelope) are ultimately shaped by individualized factors, such as muscle strength and neuromuscular control, allowing for personalized assessments of balance capacity (22). This envelope of the BR establishes the limits of an individual's balancing ability and can be used to extract specific features, such as the area of the BR. Previously, optimization-based approaches were implemented to numerically determine the BR using kinematic models (23, 24, 25) by iteratively testing the balance recoverability of specified initial COM states, where experimental validation was performed on bipedal robot systems and some human studies. A reinforcement learning (RL)-based muscle controller was also previously developed to investigate balancing ability in simulation using BRs, which demonstrated distinct differences in BR shapes and areas between healthy and pathological musculoskeletal models, showing promise for quantifying balance (26). The RL-based approach builds upon optimization-based methods by utilizing a musculoskeletal model in lieu of traditional kinematic modeling, allowing for the exploration of physiological effects on balancing ability. While the use of musculoskeletal models increases the real-world relevancy of simulations, there is still a need for further experimental validation of the resulting outcomes. Although the aforementioned computational approaches exist for whole-body balance assessment using BRs, empirical studies are limited in number and a clear application of BRs in real-world settings has not yet been outlined.

In this study, we aimed to establish a COM-based balance analysis approach using experimentally derived BRs to quantify an individual's ability to maintain balance during controlled dynamic sway exercises. Through this, we sought to validate the use of whole-body COM-based balance assessment parameters, such as the BR area, by comparing existing LIP- and COP-based metrics and associated joint patterns. As a result, the proposed analysis represents one of the few existing multi-dimensional balance quantification efforts, in which biomechanical parameters of different nature (e.g., COP-, COM-, joint-based) are contextually analyzed. We believe that the MoS and BR complement each other by providing distinct but related insights: MoS offers immediate feedback on balance risks and corrective actions, while BR provides a more comprehensive picture of balance capacity over time, accounting for individual variability. However, unlike traditional LIP- or COP-based metrics, our BR approach captures the COM state space trajectories from real-world dynamic sway, providing a more complete measure of balance ability. Furthermore, we conducted a sub-analysis of sex-specific differences in the COM, BR, COP, and inverse kinematics (IK) outcomes, contributing to a deeper understanding of individual variability in balance control, offering potential considerations for more individualized rehabilitation programs.

RESULTS

A demographic summary of the participants is presented in Table 1. Male and female groups were compared in the following measures: age, height, body mass, body mass index (BMI), and foot length. There was no significant difference in age between male and female participants (p=0.7657). However, participant height and body mass were significantly greater in male participants (p<0.001 and p = 0.0128, respectively). BMI was not significantly different between the male and female participant groups (p = 0.4779). Lastly, foot length was found to be significantly longer in males than in females (p<0.001). Overall, expected sex differences (height, body mass, and foot length) were present between the two groups; however, age and BMI were not significantly different.

Table 1 Participant Demographics Summary

	All Participants (N = 22)	**Male Participants (N=11)**	**Female Participants (N=11)**	***p*-value**
Age (yrs)	24.77 ± 4.37	24.82 ± 5.15	24.73 ± 3.69	0.7657
Height (m)	1.72 ± 0.13	1.82 ± 0.07	1.62 ± 0.09	**<0.001***
Body Mass (kg)	71.48 ± 17.11	80.70 ± 15.70	62.28 ± 13.50	**0.0128***
BMI	23.92 ± 3.80	24.23 ± 3.78	23.62 ± 3.99	0.4779
Foot Length (m)	0.25 ± 0.02	0.268 ± 0.016	0.237 ± 0.018	**<0.001***

*denotes significance (p<0.05). Values presented are mean ± standard deviation.

Balance Region Analysis

For the balance recovery analysis during the supported and perturbed sway trials, the hand contact phase was excluded to reduce the influence of potential external assistance. To quantify hand contact contribution, F_{push} was calculated for all trials to establish a force threshold for identifying instances of hand contact (Fig. 7). After comparing force profiles across all participants and examining the videos of hand contact and separation, a threshold of ±30 N (sign dependent on direction of the pushing force) was used to determine hand contact. This comparison was performed by matching the moment of hand release with the reduction in external force (calculated by the force balance in Eq. 1); 30 N was empirically found by averaging the residual force without hand contact across multiple sessions and participants. After determining the force threshold, the COM states without hand contact were extracted for the supported and perturbed conditions and included in the analysis, along with all COM states from the voluntary sway exercise. Here, all COM state trajectories without hand contact in the direction of recovery are referred to as balance recovery trajectories and are included in the corresponding participant- and task-specific BR. For voluntary sway, the entire trial was considered to be a test of balance recovery, so all oscillating COM state trajectories in both directions were included in the BR. COM states from voluntary sway, supported sway, and perturbed sway trials for each participant were used to obtain the participant-specific BRs, encompassing all five activities (VS, SSF, SSB, PSF, and PSB). All states were then normalized to facilitate direct comparison between participants, where the COM position was normalized by the foot length along the sagittal plane (L_{foot}) and the COM velocity was normalized by $L_{foot} \times \omega$, with ω as the natural frequency of the participant's LIP model (21). The original and normalized BRs of two example participants are shown in Fig. 1.

Considering all participants' respective BRs [see Additional file 6 for all BRs], the COM states stayed within the analytical boundaries provided by the LIP model (using their respective height and foot length) during the VS exercise (blue). COM states during SSF and SSB also generally stayed within the analytical limits; though, in some cases, the participants were able to reach the edges of their BoS in the supported condition. In the perturbed trials, the added velocity component from the push can be observed in the BR with greater velocities than the other sway exercises, where the balance recovery COM trajectories also generally stay parallel to the characteristic direction of the LIP boundaries (23), hence resembling the balance recovery of an LIP model.

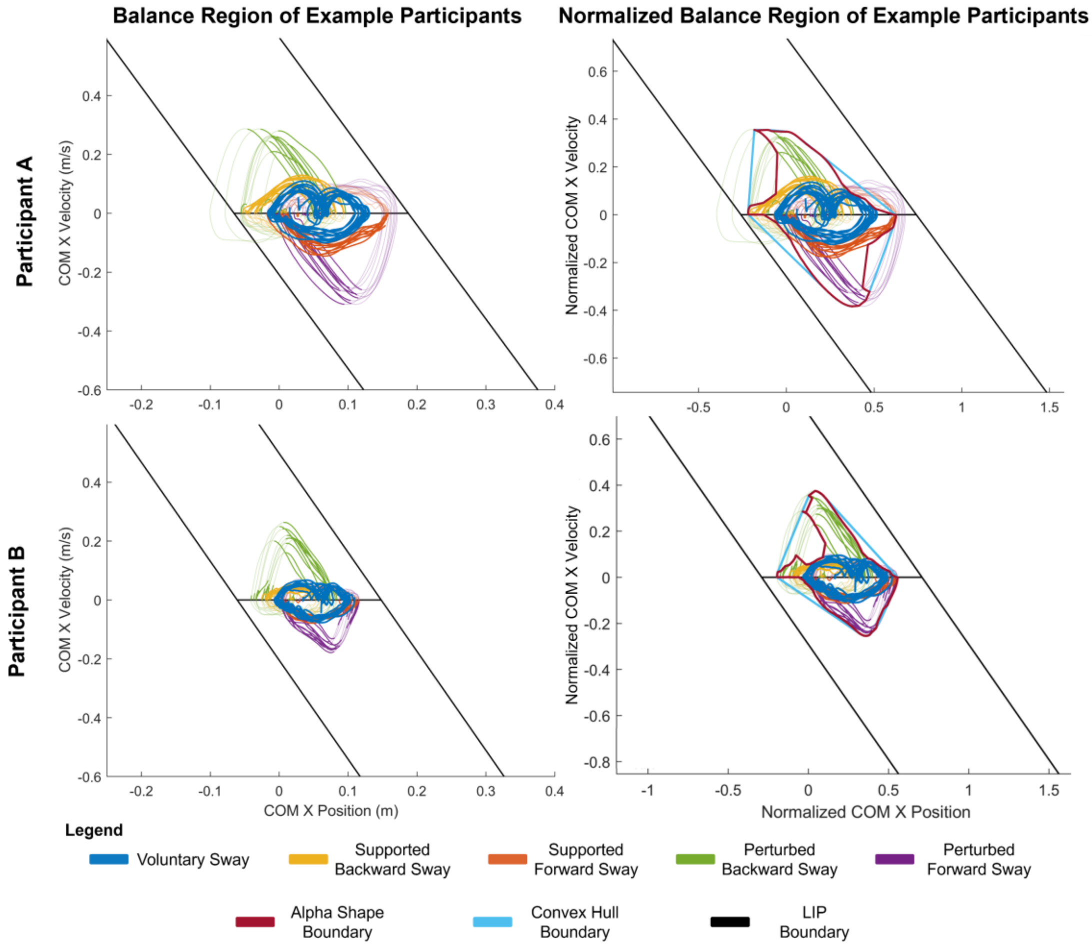

Figure 1 Original (left column) and normalized (right column) BRs of two example participants (one per row) are presented, where voluntary sway is blue, supported forward sway is red, supported backward sway is yellow, perturbed forward sway is purple, and perturbed backward sway is green. The analytical LIP boundaries are presented as two black lines, and the effective BoS (from marker positions of the heel and toe) of the participant is also presented in black with the participant's ankle position at x = 0 (calculated from body kinematics). All COM positions are with respect to the ankle position. Thick lines indicate the balance recovery portions of the exercise when there is no external support or pushing forces applied (based on the force threshold), and the lighter lines are the remaining COM states of the entire trial. In normalized BRs, the COM position was normalized by the foot length (L_{foot}) and the COM velocity was normalized by $L_{foot} \times \omega$.

For each participant, the selected COM-based metrics were derived from the normalized BRs (Fig. 2, Table 2). Significant differences between sexes were observed in the overall maximum posterior MoS metric (p=0.01974, effect size=1.081). Similarly, both the total XcoM range and XcoM range from MoS_0 were significantly different between sexes (p<0.0392, effect size=0.833±0.119). Lastly, both alpha shape and convex hull area metrics presented significant sex differences (p<0.045, effect size=0.585±0.007). All other COM-based metrics did not reveal any significant differences between the two groups.

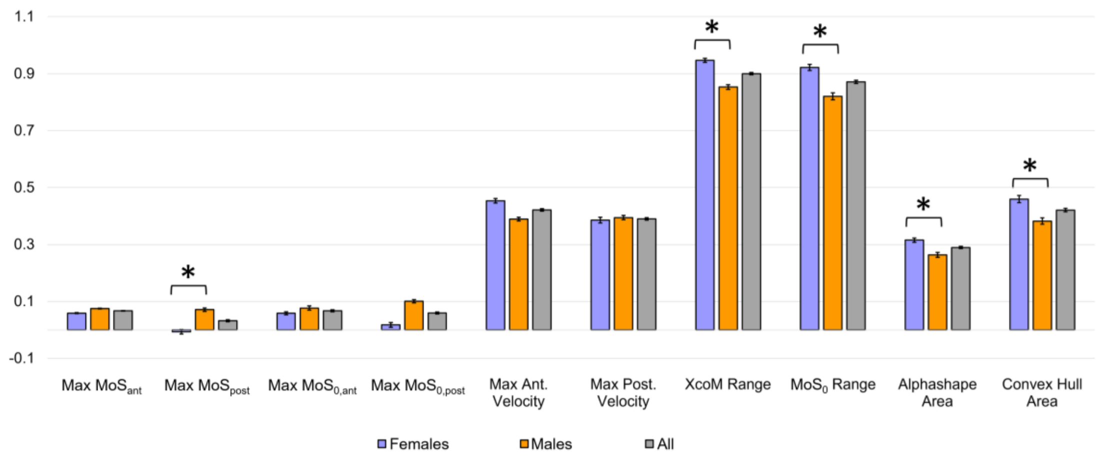

Figure 2 Normalized COM- and BR-based metrics across all participants and groups. The y-axis is the non-dimensional value for each metric. *denotes significance (p<0.05).

Table 2 Normalized COM- and BR-based metrics

	All Participants (N=22)	Male Participants (N=11)	Female Participants (N=11)	p-value	Effect Size (Cohen's d)
Maximum MoS_{ant}	0.067 ± 0.077	0.076 ± 0.066	0.059 ± 0.089	0.6294	0.209
Maximum $MoS_{0,ant}$	0.068 ± 0.076	0.077 ± 0.062	0.059 ± 0.090	0.6551	0.236
Maximum MoS_{post}	0.033 ± 0.080	0.071 ± 0.083	-0.006 ± 0.058	**0.0197***	1.081
Maximum $MoS_{0,post}$	0.060 ± 0.089	0.101 ± 0.073	0.018 ± 0.087	0.0590	1.031
Maximum Anterior Velocity	0.422 ± 0.099	0.389 ± 0.083	0.454 ± 0.107	0.1313	0.671

Maximum Posterior Velocity	0.390 ± 0.084	0.395 ± 0.091	0.386 ± 0.080	0.9096	0.104
XcoM Range	0.900 ± 0.132	0.853 ± 0.133	0.947 ± 0.118	**0.0055***	0.749
MoS_0 Range	0.871 ± 0.120	0.820 ± 0.121	0.922 ± 0.100	**0.0392***	0.917
Alpha Shape Area	0.290 ± 0.092	0.264 ± 0.096	0.316 ± 0.083	**0.0357***	0.580
Convex Hull Area	0.421 ± 0.134	0.382 ± 0.122	0.460 ± 0.139	**0.0450***	0.590

*denotes significance (p<0.05). Values presented are mean ± standard deviation.

COP Metrics

Task-specific differences in COP were assessed using an rmANOVA for each of the selected COP measures; significant differences were found in the RMS, 95% confidence ellipse area, and mean velocity in the AP direction (p<0.0205). COP range in the AP direction did not reveal significant task-specific differences. Post-hoc paired t-tests between tasks for RMS revealed significant differences between VS and SSB, VS and PSF, VS and PSB, SSF and SSB (p<0.001), SSF and PSF, SSF and PSB (p<0.0029). The paired t-tests between tasks for area of the 95% confidence ellipse revealed a significant difference only between the VS and PSB (Fig. 3B, p=0.0039) activities. Among the task comparisons for mean velocity, significant differences were found between VS and SSB, VS and PSF, VS and PSB, SSF and PSF, SSF and PSB, SSB and PSF, and SSB and PSB (p<0.0019). Outcomes of all post-hoc task comparisons can be found in Additional file 7. Considering sex differences, the only significant difference between male and female participants was found in the COP range metric during the PSB (p=0.0305).

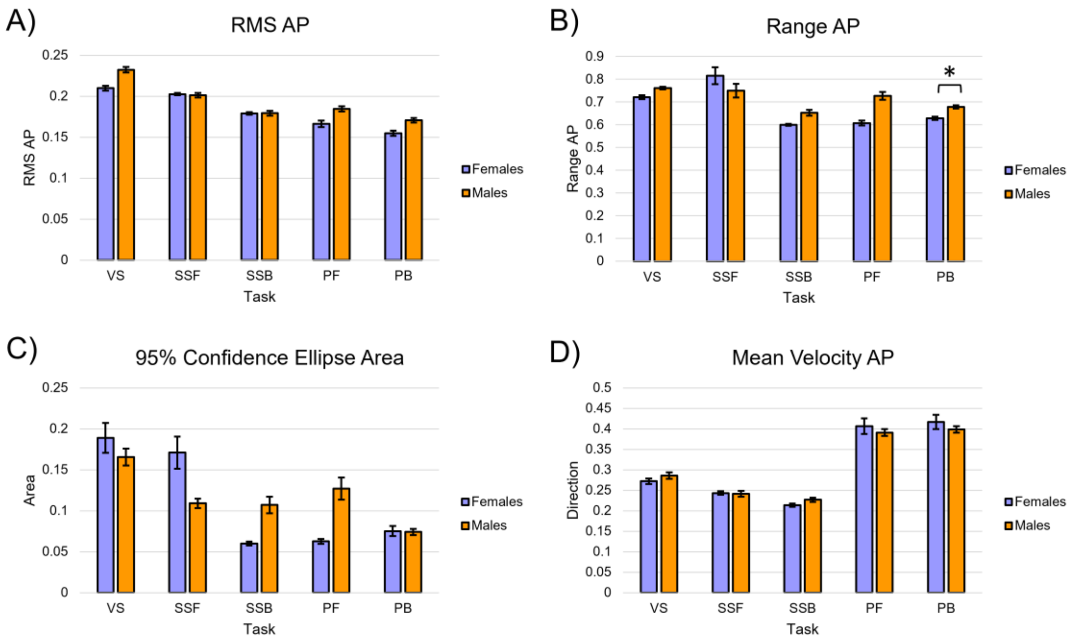

Figure 3: Mean of selected normalized COP metrics for each group with sex-specific comparison shown. Error bars represent standard error of the mean. The y-axis is the non-dimensional value for each COP metric. *denotes significance ($p<0.05$).

Inverse Kinematics

To consider the joint angle trajectories during the sway exercises across all participants and repetitions, each sway activity was divided into different phases, depending on the different postures present in each activity (Fig. 4). For each trial, the COM velocity zero-crossings were used to determine the key postures, and all joint angles were resampled to match the phase, where each phase was set to be 200 samples; after the resampling, all repetitions were then averaged for each participant. This breakdown allows for a more direct comparison between the activities, the overall balance capacity given by the BR metrics, and the different joint-level mechanical strategies for postural balance observed from IK results.

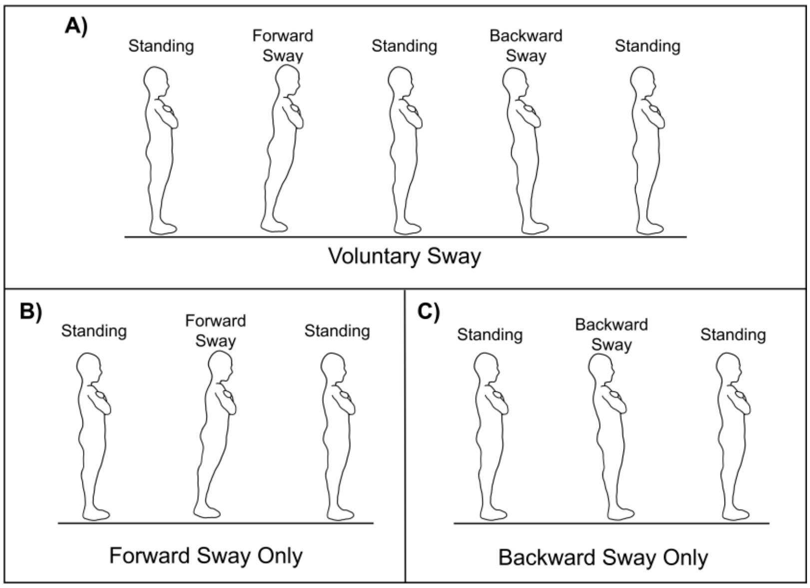

Figure 4 Phase definition for sway activities. **A)** The voluntary sway exercise involved participants starting from a standing posture, swaying forward, returning to standing, swaying backward, then returning to standing again. **B)** The activities involving a forward sway only (supported forward sway and perturbed forward sway) were segmented into standing, forward sway, and return to standing. **C)** Similarly, activities involving a backward sway were composed of an initial standing posture, backward sway, and the recovered standing posture.

The sagittal plane IK results for five joints (pelvis with orientation relative to global frame, lumbar, hip, knee, ankle) are presented in Fig. 5, where the lower-limb joint (hip, knee, ankle) are from the right side of the body, assuming symmetry during the tasks. Although the OpenSim model comprised joints across the entire body and all joints were used for the IK calculations, the primary lower-limb, lumbar, and pelvis joints controlling sagittal plane movement were selected for the descriptive IK analysis and plotting. Additional figures for female and male participants separately can be found in Additional file 8. There was an increased anterior pelvic tilt during the forward sway portion of the voluntary sway activity, as well as both supported and perturbed forward sway activities. Similarly, the pelvis had increased posterior tilt during the latter half of voluntary sway, which involved swaying backward, and both isolated backward sway activities. The lumbar joint (connecting the lumbar segment and the pelvis) stayed relatively constant across all activities, except for a slight increase in flexion at the onset of pushing during the perturbed backward sway activity. Considering the starting posture across all activities, IK results indicate that participants had increased hip extension while standing. During the first half of voluntary sway, there was an increase in hip flexion, which was also observed in both the supported and perturbed forward sway activities; likewise, the latter half of voluntary sway and both backward sway activities had increased hip extension. Knee extension increased during all forward sway motions, and knee flexion increased during the backward sway motions. Across all activities, the ankle joint remained in a slightly dorsiflexed position. However, unlike the more proximal joints in the kinematic chain, the ankle joint did not present a consistent pattern across forward and backward sway movements. For instance, the overall pattern of increased plantarflexion then increased dorsiflexion was present during both voluntary sway and backward sway. There was increased dorsiflexion then plantarflexion during the supported forward sway activity, but overall slightly increased and constant dorsiflexion during the perturbed forward sway activity. The ankle joint also presented increased variance across trials and participants during the pushing region of the perturbed backward sway trial. Overall, the isolated forward and backward sway IK results closely resembled those of the forward and backward sway components of the voluntary sway activity.

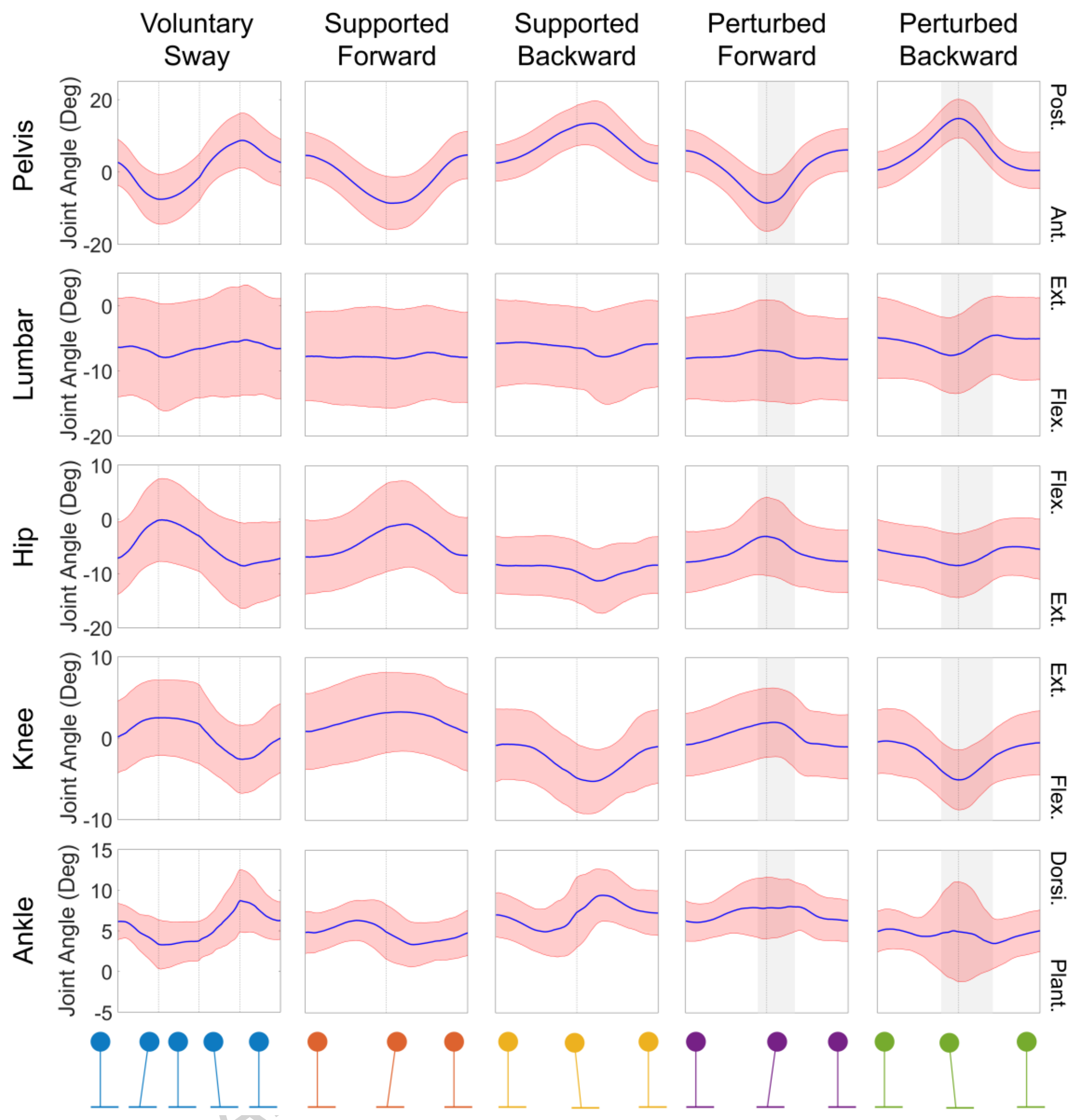

Figure 5 IK trajectories for pelvis, lumbar, hip, knee, and ankle joints from all participants are shown for all five sway activities during each phase segmentation. Assuming symmetry, lower-limb joints (hip, knee, ankle) from the right side are presented. Mean ± standard deviation is shown, where standard deviation is represented by the red shaded region. Light gray regions indicate portions of the perturbed trials where hand contact was found to be above the specified threshold. Stances used for each activity phase are represented at the bottom of the figure; colors for each stance match legend in Fig. 1.

DISCUSSION

Many existing balance assessment metrics are not implemented in a comprehensive manner and fail to capture information from the whole-body balancing ability; instead, most are focused on the foot-ground interaction and simplified models of human balance. Therefore, there is a clear need for more holistic approaches that account for the coordinated whole-body movement required to regain and maintain balance, particularly in the field of physical rehabilitation. To address this gap, the present study aimed to establish a more comprehensive approach with an experimental balance assessment framework for large dynamic postural sway that employs COM-, BR-, and COP-based metrics using a standard motion capture setup. This framework was exemplified by investigating balancing ability during five sway activities performed in the sagittal plane: voluntary sway, supported forward and backward sway, and perturbed forward and backward sway. Similarly, sex-specific differences across selected balance metrics were also compared to demonstrate examples of insights that can be gleaned from this approach. Lastly, the IK results from these activities were compiled and compared for joint-level differences across tasks and sexes.

Assessment of BR Metrics and Comparisons with LIP Boundaries

LIP models are widely used to approximate bipedal motion (27) and do well in designing simple balance controllers, particularly in robotics (28, 29); additionally, the MoS criterion based on the LIP model is a well-established metric in clinical balance assessment (30). However, these models can fall short in capturing the unique nuances during balance recovery, particularly with humans. Though there is limited exploration of changes to the BR of humans in experimental settings, robot applications have demonstrated that real-world balancing ability can extend beyond the LIP boundaries (31, 32). Although these LIP modeling approaches can be generalized to all bipedal systems, humans' neural responses and soft tissues, among other factors, introduce unique considerations. To this end, experimental studies can help elucidate the shortcomings of kinematic models and help inform future avenues for developing more detailed bipedal models and more accurate metrics. In the presented study, participants generally maintained their balance within the analytical LIP boundaries, with minor excursions outside of the effective BoS in the sagittal plane. Across most tasks, average anterior and posterior MoS metrics demonstrated positive values, indicating that participants were able to maintain their balance within the LIP limits. The findings from this study also contribute to the current literature on the utility of using MoS and XcoM for balance assessment.

However, the overall shape of the BR regions defined here presented unique outlines that can be bypassed with standard simplified balance metrics. Here, alpha shape and convex hull were both used for determining the outline of the BR and calculating its area, which can be used to draw inferences regarding differences in balancing ability or task performance. Similarly, the BR and its derived metrics provide insight into an individual's balance capacity, allowing for its area to provide a trackable metric of overall balance. Although both the alpha shape and convex hull area metrics are effective at distinguishing sex differences in this study, the meaning of their resultant areas may vary; the boundary outlined by the alpha shape is more sensitive to the individual points on the COM state trajectories, which can be adjusted through the desired alpha parameter, while the convex hull better represents the outermost points of the entire collection of COM states. The sway activities here were selected to maximize exploration of a participant's BR and increase the number of successful

COM states, but they may not have been able to capture that participant's entire BR area. To increase exploration further and potentially expand the sagittal plane BR, more sway exercises in other directions (e.g., diagonal, mediolateral) could be included. Due to the differences in the two area polygons, the convex hull may provide a better estimate of the participant's overall BR area, since it provides a more generalized estimation. However, with sufficient sway exercises and trials, the alpha shape boundary could eventually capture the BR area more accurately, since the alpha shape's boundary is primarily determined by COM states traversed by the participant. In addition, as a future avenue of research, quantifying the convex hull area residing outside of the LIP region could provide a metric of dynamic activities and how much balance ability is challenged.

Previously, we developed a balance controller in simulation using real-time muscle control of a musculoskeletal model through reinforcement learning, where BRs were determined for several model configurations (26). In our computational approach, we outlined that a BR should encompass all COM states along a balance recovery trajectory, not just initial COM states, due to the time-dependent changes that muscle undergoes while performing actions; similarly, in this experimental work, we included the full balance recovery trajectories of each trial. We also found that the full range of the BoS was included within the BR when considering the whole balance recovery trajectory. In the experiment, however, the full BoS range was primarily covered during the supported trials for most participants. This is potentially due to other neural responses (e.g., subconscious postural reflexes, fear of falling, perceived instability) in the participants preventing them from reaching their BoS limits on their own, which are not present in the musculoskeletal model framework. When comparing the

BR outcomes of both the computational and experimental approaches, the computational approach was able to reach larger COM velocities and total BR areas than the experimental outcomes. This is likely due to the scale of perturbations applied during the experiment trials; if a different perturbation method (e.g., treadmill, sliding platform) were to have been utilized, larger perturbations could be applied at varying increments of magnitude, allowing for a wider range of COM velocities. In future work, comparing the outcomes across a selection of different perturbation methods would be an interesting way of achieving a standardized protocol for BR generation and balance assessment.

In higher-order kinematic and dynamic models, it is expected that mass distributions of each rigid body link will affect the whole-body motion and outcomes; similarly, a person's mass distribution would affect their balancing ability and overall kinematics, which was a primary motivator for using musculoskeletal models to determine COM kinematics in this study. Sex-specific differences in humans typically arise from differences in mass distribution and kinematic factors (e.g., joint angle limits), which can also then be complicated by dissimilar aging patterns (33, 34). However, reduced-order models like the LIP are unable to account for these effects due to their point mass assumption. To this end, to bypass the increased complexity of higher-order models, many researchers and clinicians prefer simple, experimentally derived metrics that can indirectly account for these differences. In the current literature, most existing sex-specific considerations in postural balance are primarily focused on COP metrics from quiet standing (35); for instance, older men were observed to have a larger COP sway area in comparison to older women (36). The need for further investigation into sex-related changes in balance and postural control through an expansive large-cohort study is highlighted in the literature, with investigations in developing children and adolescents (37, 38, 39) and older adults (36, 40, 41, 42, 43). Through this work, we aimed to contribute to the literature on sex-specific changes in balance by providing insight into how the BR-, COM-, and COP-based metrics vary between groups, as well as variations in general IK trends.

We initially hypothesized that no significant sex differences would be present in this sample, since participants comprised healthy young adults and that the normalization of COM states would adjust for sex-specific differences (e.g., height, body mass) in the resulting metrics. Interestingly, female participants presented increased MoS in the posterior direction when compared with male participants, but no differences in the posterior MoS_0. Similarly, both the XcoM range and XcoM range obtained from MoS_0 also presented sex-specific differences, where female participants demonstrated greater range than male participants. However, since separating the participant pool into two sex groups yields 11 participants in each group, these sex comparisons should be considered exploratory at this stage and should guide future work.

Additionally, a portion of these results could potentially be influenced by participants' fear of falling and trust during the session; although we did not collect any subjective measures, psychological effects may have been present to a certain degree while participants performed the task. For instance, swaying maximally backwards can be intimidating due to the lack of visual feedback, and requesting participants to rely on their ankle joints to regain balance may have increased the fear response in participants; recent work has demonstrated the link between fear of falling and backward sway in older adults, affecting their postural control strategies (44).

Visuospatial feedback during balance tasks has been highlighted in the literature and a strong link between the visual and motor systems has been demonstrated, among other physiological systems (45). In particular, the use of virtual reality has shown to be an interesting avenue for investigating the effect of visuospatial feedback on balance, with existing work demonstrating that artificially modifying the surroundings can elicit anxiety-related changes in balance (46). Although there is limited work on physiological feedback during postural sway, similar approaches using heart-monitoring and the use of virtual reality could provide interesting avenues for future research on the fear of falling in individuals. Fear of falling is of particular importance when considering older adults and individuals with mobility difficulties (44, 47, 48, 49), thereby reducing their overall quality of life and independence.

Influence of Task and Sex on COP Metrics

Among the selected COP metrics, RMS, 95% confidence ellipse area, and mean velocity in the AP direction presented significant differences across the performed tasks; this difference indicates that the selected sway exercises were sufficient to affect the COP measures and elicit responses. RMS, area, and mean velocity have been shown to be sensitive to distinguish between fallers and non-fallers, as well as determining fall risk (14). Unexpectedly, COP range did not present significant differences across the tasks. COP range was initially selected as a metric of interest because we anticipated that varying the direction and magnitude of postural sway would directly affect the maximal COP excursions in the anterior and posterior directions. In particular, posterior sway can create greater instability due to the limited BoS in the posterior direction and the differences in neural processing of forward and backward perturbations (50).

Upon visual inspection, several tasks seemed to have sex-specific differences, but these differences were not reflected in the statistical analysis of the COP measures' sex comparisons. One reason as to why these observed trends were not found to be significant could be that the study was underpowered due to the small sample size; although the participant pool was sex-balanced, a larger sample size could help to better determine whether these trends could be statistically significant. To check for achieved power and determine whether sample size was limiting the analysis, a power analysis was performed for all four COP metrics' rmANOVA models. These power analyses showed that the sample was underpowered for both the COP range and area metrics by achieving 50-55% power for both parameters; however, the RMS and mean velocity were found to have more than 95% power. Considering that the sample was underpowered for some of the COP metrics, sex comparisons should be considered exploratory at this stage. Among the COP metrics, the only sex-specific difference found was in COP range during perturbed backward sway. Using the COM-based metrics as a guide, the COP range would have been expected to demonstrate sex-specific differences, but it was unexpected that this difference was only evident in the perturbed backward sway condition. This observation may be somewhat aligned with the COM metrics' results since the MoS in the posterior direction was also found to be significantly different between sexes, indicating that both the COP and COM metrics demonstrate differences in balancing ability during posterior sway, but this comparison was not fully determinable here. Similarly, the area metrics for the COM presented sex-specific differences, while the COP area was not significantly different amongst the groups; however, considering the visible trends in Fig. 3, further testing with a larger sample with stronger power may provide a better representation of the COP metrics.

IK Patterns and Resulting Effects on BRs

Among the five joints of interest, the pelvis (related to global frame), knee, and ankle joints showed the greatest deviations during the tasks, while the hip joint varied primarily during the voluntary and forward sways; the lumbar joint remained fairly consistent during and across all tasks. The ankle demonstrated expected plantarflexion during forward sway and dorsiflexion during backward sway, consistent with sagittal-plane balance control assumptions. However, deviations in ankle angle were reduced during the perturbed trials, potentially reflecting more conservative balance recovery. During backward sway tasks, the knee presented greater flexion, while the changes in knee angle were less pronounced during forward sway tasks. This observation is consistent with prior reports of increased knee flexion during balance recovery from perturbations (51). Similarly, in (51), the ankle demonstrated plantarflexion and the hip experienced extension, which correlated with the patterns shown in Fig. 8. For forward sway, the observed increases in ankle plantarflexion, knee flexion, hip flexion, and anterior pelvic tilt are consistent with prior reports of sagittal-plane balance recovery (52). Similarly, the hip joint had increased flexion during the voluntary and forward sway tasks, and trends were less pronounced during backward sway. Maximum hip flexion occurs during the beginning of the recovery phase in the forward sway tasks, which may be a strategy to generate enough momentum to initiate recovery.

While the BR provides a compact, COM-based representation of whole-body balance capacity, it does not explicitly encode the joint-level strategies used to achieve the observed COM states. However, the abovementioned IK results suggest that the shape and directional extent of the BR emerge from the availability and coordination of underlying joint strategies. In particular, the greater anterior extension of the BR observed across tasks is consistent with the use of coordinated proximal strategies during forward sway, including increased hip flexion, anterior pelvic tilt, and knee extension. These multi-joint contributions allow forward COM displacement to be achieved without excessive reliance on ankle torque, thereby enabling participants to access a larger range of anterior COM positions and velocities while remaining recoverable. In contrast, posterior sway was associated with increased knee flexion, hip extension, and greater variability at the ankle, particularly during perturbed backward sway. These patterns reflect the biomechanical and sensory constraints of posterior balance control, where limited ankle dorsiflexion capacity and reduced visual feedback restrict the robustness of available recovery strategies. As a result, the posterior BR was consistently more compact, with reduced margins of stability. Taken together, these findings suggest that BR geometry reflects not only COM dynamics but also the functional availability and robustness of joint-level balance strategies, with asymmetries in BR shape encoding directional differences in postural control mechanisms that are not directly observable from COM-based metrics alone.

While this was unintended, the reliance on other joints to compensate for limitations at the ankle joint goes to show that a single-joint model would face difficulty representing bipedal balance. To this end, COM states from an LIP model would be insufficient to fully capture the COM kinematics from a higher-order system (e.g., humans). However, it should still be noted that the LIP model presents great utility in developing simple and easy-to-implement solutions for quick bipedal analysis and control, which helps maintain its prevalence.

When considering sex-specific differences in the joint angle trajectories, general trends among all tasks and joints remained similar across both groups. Interestingly, there seemed to be increased variance in the ankle joint in female participants during perturbed backward sway, particularly during the region where the perturbation was applied and hand contact was maintained with the participant. This ankle variance could be also attributed to reduced ankle stiffness in females (53), as well as increased ankle joint laxity (54). However, for all other joints, both groups presented similar trends across all tasks, with female participants presenting slightly reduced variation in joint angles. These findings, in conjunction with the sex differences observed in the COM-based metrics, may reflect known biomechanical differences in ankle stiffness or risk perception between sexes and point to the need for sex-specific rehabilitation protocols.

Limitations

While the presented balance assessment approach demonstrates advancements in the field of balance rehabilitation, several limitations need to also be considered for the overall conclusions and clinical feasibility. First, the study wholly comprised healthy young adults, limiting the extrapolation of results to any specific balance decline resulting from a condition, such as in healthy aging or neurological disorders. Although the primary aim of this study was to establish a methodology for balance assessment using experimental approaches, further investigation including a cohort of individuals with a specific balance limitation (e.g., older adults) would improve the work. Alternatively, the equal number of male and female participants allow for sex-specific comparisons, which are briefly explored in this work; however, the limited number of participants in each group reduces the robustness of the findings, and future work should address this limitation by increasing the number of participants to achieve adequate power. Alongside the increase in participants, a linear mixed-effects model (LMM) could be employed as future statistical analysis to better handle imbalances in the data as more participants are included in the dataset. Additionally, the task and protocol design could be a limitation due to potential learning effects and perception of safety by the participants. Each activity was performed for 10 consecutive repetitions, which may have influenced the final repetition of the activity by improving performance due to learning; though, this was performed as such to increase the number of COM states and to replicate the computational approaches. During these activities, the participants may have also limited their sway due to a fear of falling, and using an overhead safety harness instead of rigid bars may help reduce these effects. In future work, the perceived safety and fear of falling should be quantified and an overhead safety harness should be used to compare possible effects of having a safety mechanism; when including individuals with balance disorders, a safety harness should be used regardless. Additionally, these five sway activities may not have been enough to capture the entire BR of each participant, and various other sway exercises should also be included to expand the breadth of COM states collected. Similarly, the BR may be influenced by the perturbation characteristics used in the assessment (e.g., magnitude, type of perturbation), thereby creating a task-dependent relationship. This potential task-dependent relationship of the BR could be explored in future work by implementing study protocols that systematically account for varying perturbation magnitudes, directions, and types (e.g., pulling/pushing, sliding). The resulting BRs from these protocols could then be compared and used to further validate the BR approach, as well as account for task dependency. To this end, further research on balance in the mediolateral direction using the presented COM-based methods should also be pursued to supplement the anteroposterior focus of this work and better characterize balance as a whole. Lastly, the external force applied from hand contact was estimated and not directly measured, thereby influencing the pushing force threshold used in the determination of which COM states to include in the final BR.

Implications for Clinical Applications

The methods presented in this study can be used synergistically with existing standard protocols to enhance balance assessment and rehabilitation programs in clinical and athletic settings. By integrating the quantification of BRs and tracking COM movement, clinicians, physical therapists, and athletic trainers can gather measurable insights into the current status and progression of individuals in their care. In particular, with the growing adoption of markerless motion capture technologies, simple video cameras can be used to track movement during sway exercises and allow for the generation of BRs without the need for expensive motion capture equipment (55, 56). While motion capture provides critical information about balance and a person's overall movement ability, integrating force sensing (e.g., instrumented insoles (57), pressure mats (58)) with motion capture also provides beneficial information regarding the dynamics that could be used to enhance balance assessment approaches. Similarly, motion capture utilizing portable and affordable inertial measurement units (IMUs) would also be a viable avenue for tracking COM motion and obtaining an individual's BR for balance assessment. To this end, open-source technologies like OpenSense (59), provided through OpenSim, allow for the integration of IMUs with musculoskeletal models directly, which would improve the expansion of the presented study in a more accessible and mobile manner. Additionally, by providing a personalized BR envelope describing an individual's balance ability, the BR may serve as a more comprehensive indicator of fall risk or rehabilitation progress than currently available clinical assessments. These personalized and measurable outcomes could supplement existing standard balance assessment protocols by providing a direct quantification that can then be compared and associated with existing outcomes (e.g., BR area vs. Mini-BESTest score). Lastly, this platform can also be expanded to develop COM tracking games using wearable sensors to provide gamified training programs for balance rehabilitation, where patients can perform exercises in an engaging manner (60). A gamified solution would also provide patients a way of assessing and training their balance both in and out of the clinic, thereby increasing the treatment dose of their treatment plan.

CONCLUSIONS

This study introduced a novel experimental approach to evaluate postural stability using participant-specific BRs derived from COM trajectories during dynamic sway. By combining full-body motion capture with musculoskeletal modeling, our approach quantified balance capacity based on COM measures by bridging standard experimental biomechanics methods and dynamic stability analyses with potential for clinical applications. Through prescribed large postural sway exercises, kinematic data were used to measure and assess balance by generating participant-specific BRs comprising COM state trajectories from successful trials across all exercises. COM states from these BRs were then compared with analytical LIP boundaries to derive and analyze several metrics (e.g., MoS, XcoM range). Participants were overall able to maintain their COM trajectories from all exercises within the LIP bounds, and were also able to extend beyond the LIP bounds in some instances, particularly during supported sway; this highlights the BR approach's utility in identifying task- and participant-specific variations in balance that traditional balance metrics would struggle to capture. Additionally, sex-specific differences were observed in the maximum posterior MoS, both XcoM range metrics, and both BR area estimations. COP results demonstrated significant task differences in the RMS, 95% confidence ellipse area, and mean AP velocity. Lastly, IK results demonstrated slight hip flexion during forward sway, potentially indicating the difficulty of an ankle strategy for balance recovery from forwarding leaning. These findings highlight the importance of joint-specific actions and interventions in balance training and rehabilitation. Overall, our methodology provides a new experimental method to assess whole-body balance during large postural sway and is presented alongside traditional objective balance measures. Future work can further investigate age- or disease-related decline in balance using the BR approach and aim to establish a normative dataset of BRs for aging or various pathologies.

METHODS

Participants

Healthy adults aged 18-60 years old were recruited for this study, yielding a total of 22 young adult participants (age = 24.77 ± 4.37 years; 11 males, 11 females), and were asked to perform a collection of balance tasks. All procedures were approved by the Institutional Review Board at the New Jersey Institute of Technology

(IRB#:2212027868) in accordance with the Declaration of Helsinki, and all participants provided written informed consent prior to participation. Inclusion criteria required participants to be free of neurological, musculoskeletal, or motor disorders and to self-assess as healthy. Exclusion criteria included diagnosed movement, neurological, psychological, neuromotor, or musculoskeletal disorders, as well as recent muscle over-strain or injury.

Experimental Setup and Balance Exercises

For each participant, 57 reflective markers were placed on specified body landmarks by trained lab personnel with extensive motion capture experience according to the Biomech 57 Marker Set (61, 62) from OptiTrack (OptiTrack, NaturalPoint, Corvallis, OR USA) (Fig. 6A); marker data were collected from a 12-camera OptiTrack motion capture system (100 Hz). Additionally, to increase comfort and provide participants the choice of having an assistant of the same sex place sensors, at least one male and one female research assistant was available during each data collection session. Participants were asked to stand in two different poses for the static calibration trials: an anatomical pose (standing up straight, feet shoulder-width apart and parallel, arms by side with palms facing forward) and a T pose (standing up straight, arms raised laterally perpendicular to the body with palms facing down). After the static trials, eight calibration-only markers were removed for the subsequent dynamic trials according to the markerset's instructions: medial elbow (LHME, RHME), medial knee (LFME, RFME), medial ankle (LTAM, RTAM), and second metatarsal (LFM2, RFM2).

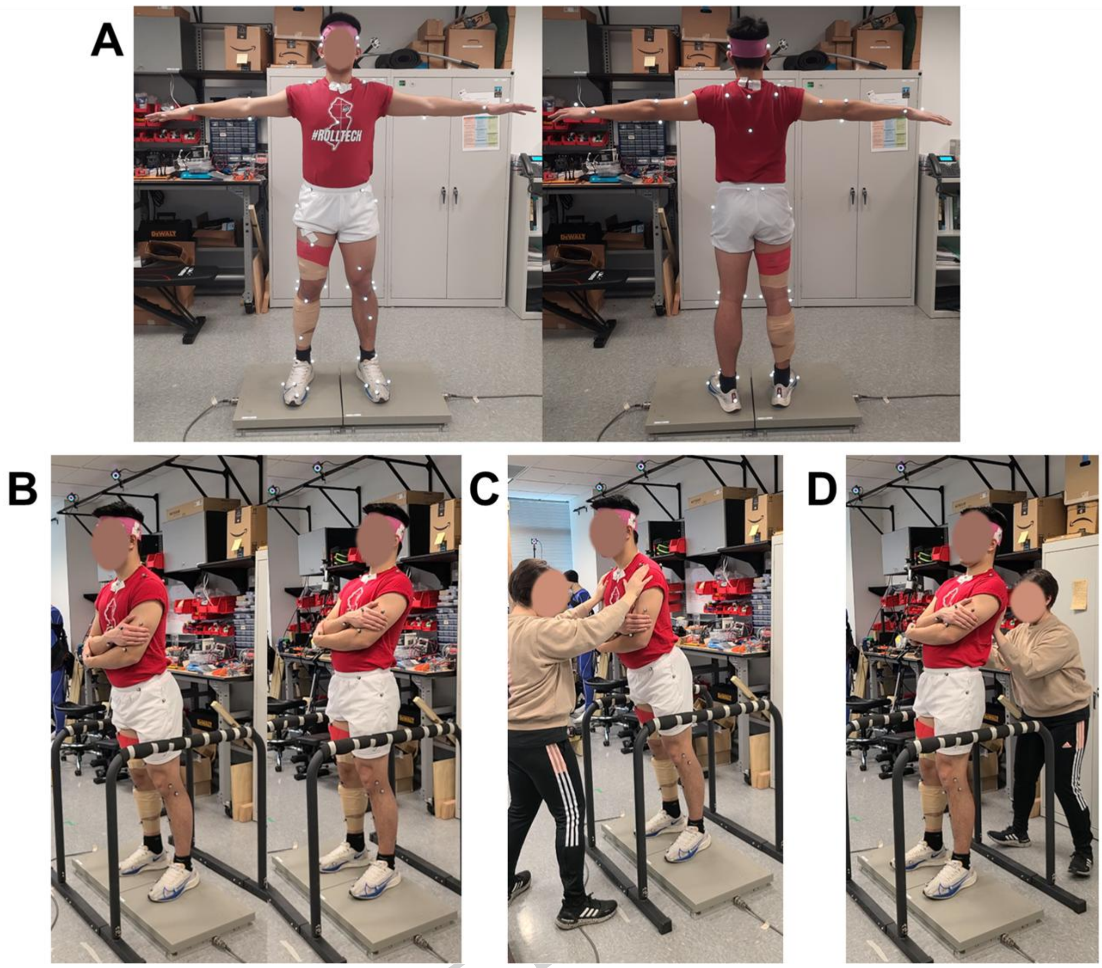

Figure 6 A) Participant standing in T-pose on AMTI (OR6-7-2000, Advanced Mechanical Technology, Inc.) force plates with 57 passive optical markers. Examples of B) Voluntary, C) Supported/Perturbed Forward, and D) Supported/Perturbed Backward Sway postures are presented.

Each participant performed ten repetitions of postural sway exercises in both anterior and posterior directions within the sagittal plane across three conditions: 1) maximum voluntary sway, 2) supported sway, and 3) perturbed sway. Additional movie files show videos of each exercise [see Additional files 1-5]. Participants were instructed to keep their arms crossed across their chest and feet flat across all exercises. During maximum voluntary sway (VS, Fig. 6B), participants were instructed to lean as far forward as possible without lifting their heels, then as far backward as possible without lifting their toes, before returning to a neutral standing position. During supported sway (SS), participants leaned forward (SSF, Fig. 6C) to their maximum extent with guidance and support from the assistant, paused, then returned to standing unassisted; the process was repeated for backward sway (SSB, Fig. 6D). For perturbed sway (PS), participants initially leaned forward (PSF, Fig. 6C) to their maximum extent with assistant support and, upon reaching peak sway, determined by onset of heel or toe lifting during sway, a controlled push in the direction of recovery was applied to induce perturbation; this was also repeated in the backward direction (PSB, Fig. 6D). This setup was inspired by the push-release test commonly used in physical therapy, and the push was applied in the direction of recovery to alter the participant's balancing ability without causing them to fall, and the primary intent was to augment the participant's velocity at the start of balance recovery. All balance exercises were executed while standing on two force plates (1000 Hz, AMTI, Watertown, MA, USA), with one foot on each force plate, from which GRF data were obtained.

OpenSim Scaling and Kinematics

A corresponding full-body musculoskeletal model (63) was anthropometrically scaled in OpenSim 4.4 for each participant using their respective static calibration pose marker data, where the musculoskeletal model comprised 29 DOFs and 92 musculotendon actuators. To do so, the Scale Tool in OpenSim was used, where the mass of the participant was inputted and "preserve mass distribution during scale" was left unchecked to prevent inaccurate calculation of the COM later. The anatomic pose marker data was loaded for the scaling, and the scaling procedure was run. Virtual marker placements on the model were manually adjusted by comparing with photos taken during the session before scaling. IK analyses were performed using the tracking data collected from motion capture to obtain the joint information throughout the trials. The overall OpenSim workflow for this IK analysis involved opening the scaled musculoskeletal model in the software, loading the marker data (.trc file) from the trial into the Inverse Kinematics Tool, and running the IK analysis. Body kinematics analyses were also performed in OpenSim to obtain the position, velocity, and acceleration of the musculoskeletal model's whole-body COM for each participant. The Analyze Tool in OpenSim was used here by loading the motion file obtained from the IK analysis and adding BodyKinematics as an analysis in the Analyses tab. The resulting BodyKinematics file describes the position, velocity, and acceleration of each rigid body, as well as the whole-body COM.

Balance Region Construction and Metrics Quantification

A BR was generated for each participant by combining the COM state trajectories from all five sway activities: maximum voluntary sway, supported forward sway, supported backward sway, perturbed forward sway, and perturbed backward sway. Drawing from the previous definitions of the analytical, optimization-based, and RL-generated BRs, experimentally derived BRs represent the area encompassing the collection of COM states during all selected sway exercises, which were obtained from the OpenSim analysis. Since the BR also aims to capture a wide range of COM states, as demonstrated in the optimization- and RL-based works (21, 26), the supported and perturbed sway trials specifically aimed to generate more extreme initial conditions that were unreachable in the voluntary sway trials for the establishment of each participant's BR.

However, during the supported and perturbed sway trials, external forces from hand contact contributed to the participant's balance recovery and influenced their COM kinematics during those instances; therefore, the COM states during the hand contact phases were excluded from the BR, which encompassed the unassisted balance capability of the participant. First, to identify COM states with hand contact, a simple free-body diagram was used to estimate the magnitude and duration of external pushing force from the hands (Fig. 7).

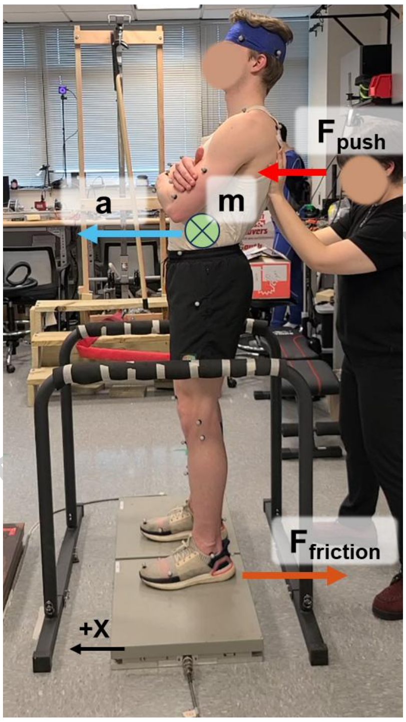

Figure 7 General free-body diagram of a participant with two external forces along the X axis: external pushing force (F_{push}) and friction force ($F_{friction}$). The total body acceleration is shown (a).

The force balance on the free-body diagram provides an estimate of the external pushing force through the following equation:

$$F_{push} = ma + F_{friction}. \tag{1}$$

where m is the participant's mass, a is the whole-body COM's acceleration calculated from the participant's body kinematics, F_{push} is the unknown force from hand contact, and $F_{friction}$ is the friction force measured by the force plate. By calculating F_{push} for each participant during the supported and perturbed trials using Eq. (1), as well as during voluntary sway should, where it is assumed that no contact with the assistant occurred, a force threshold was established to systematically identify COM states with an external force above the limit (i.e., presence of hand contact). In addition to the removal of hand contact, only COM states in the direction of balance recovery were included in the BR.

After constructing the BR, several metrics of different natures were calculated in this study to assess balance recovery ability of participants: COM-based metrics are introduced based on the constructed BR, COP-based metrics are investigated to align with established literature, and IK results are observed to study the joint contributions to balance recovery. The COM-based measures were as follows: maximum anterior and posterior MoS, maximum anterior and posterior velocity, XcoM range, area of the BR estimated using a fitted alpha shape, and area of the BR estimated using a convex hull (Fig. 8). As previously defined, the MoS is the distance between the XcoM and the edge of the BoS; here, specifically, the maximum anterior and posterior MoS were defined as the maximum distance between the XcoM and toe or heel of the BoS, respectively. Positive MoS values are within the LIP-defined boundary, while negative MoS values are outside of the boundary. Similarly, XcoM range is the distance between the maximum and minimum XcoM. In addition to the standard MoS, we also calculated the MoS for COM equilibrium states (i.e., states with zero velocity), named MoS_0, which essentially represents the distance between the BoS limits and the maximal COM positions along the zero-velocity line of the BR in the anterior and posterior directions.

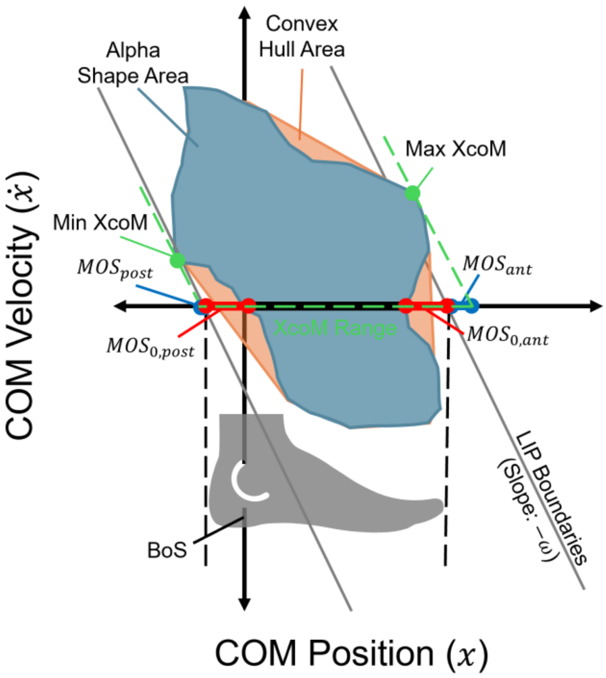

Figure 8 Representation of balance region and its corresponding metrics. XcoM and MOS metrics are presented in both the anterior and posterior directions, with MOS in blue, MOS_0 in red, and XcoM range in green. Both alpha shape (shaded blue) and convex hull (shaded orange) BR areas are shown. BoS limits are defined at the heel and toe, with x = 0 placed at the ankle joint. The LIP boundaries, defined by the relationship shown in Eq. (2), are shown as gray parallel diagonal lines with a slope of -ω.

The XcoM is often used to establish the balance stability region of an LIP model (18) and is given by:

$$XcoM = x + \frac{v}{\omega} \tag{2}$$

where x is the horizontal COM position in the sagittal plane, $v = \dot{x}$ is the horizontal COM velocity in the sagittal plane, and $\omega = \sqrt{g/L}$ is the natural frequency of the LIP, where g is the gravity constant and L is the height of the LIP. The LIP height, L, for each participant is determined by their average whole-body COM height from a 30-second standing trial. The condition of balance stability for the LIP is such that the XcoM is contained within the BoS of the legged system (18). Here, we use the maximum distance between the heel and toe markers as the functional dimension of the BoS in the sagittal plane. By equating the expression of the XcoM in Eq. (2) to the anterior and the posterior edge of the BoS, two parallel lines with a slope of -ω obtained from the XcoM definition can be found as the analytical limits of dynamic balance of the LIP model (23). These parallel lines provide an analytical basis for comparison with the experimentally derived BR, as well as a point of reference for the MoS. This LIP-based balance assessment is based on the following assumptions: a point mass model with a constant COM height, a rigid flat foot, unrestricted friction force, unconstrained ankle motion, and ankle torque indirectly regulated by constraining the COP within the BoS. Further detailed derivations can be found in (18) and (23).

The BR area was estimated by defining an envelope of the collection of COM states using two boundary estimation approaches: alpha shape and convex hull (Fig. 8). The alpha shape estimates the outer boundary of the BR using an alpha parameter (64, 65), which controls the level of shrinkage around the outer points, whereas the convex hull determines the set of all convex combinations of points in the BR to estimate the boundary (i.e., an alpha shape with $\alpha = 0$ or Inf). Here, the alpha parameter was automatically determined as the critical α using the MATLAB package to represent the tightest boundary of the BR.

Lastly, COP data were acquired from two separate force plates, one under each foot, and were normalized based on the foot length and width, as determined from the foot markers. To ensure comparability with COM-based metrics, only the COP trajectories during balance recovery without external pushing force were included in the analysis.

COP measures were calculated using the open-source code from (14), which provides standardized quantifications of common COP metrics. Selected COP measures of interest presented here include: root mean square (RMS), range, 95% confidence ellipse area, and mean velocity in the AP direction.

Statistical Analysis

Independent t-tests were conducted to assess sex-specific differences for demographical variables and COM-based metrics. Normality was evaluated using the Shapiro-Wilk test, while Levene's test was applied to assess variance equality. If either assumption failed, the corresponding recommended nonparametric tests were utilized (e.g., Mann-Whitney U). Repeated measures ANOVA (rmANOVA) models were used to find task differences in the selected COP metrics. Following the rmANOVA, paired t-tests were performed among the 10 pairwise task comparisons (VS-SSF, VS-SSB, VS-PSF, VS-PSB, SSF-SSB, SSF-PSF, SSF-PSB, SSB-PSF, SSB-PSB, PSF-PSB) as post-hoc tests with the appropriate Bonferroni correction, yielding a significance criterion of $p<0.005$. Cohen's d was used to calculate and report effect size. Subsequent sex-specific differences in selected COP metrics were assessed using independent t-tests. Statistical analyses were all conducted using R (Version 4.3.1, R Foundation for Statistical Computing, Vienna, Austria), and significance was determined using $p<0.05$.

ADDITIONAL FILES

File name: Additional file 1

File format: .MP4

Title of data: Video of Voluntary Sway

Description of data: De-identified video of a participant performing the voluntary sway activity.

File name: Additional file 2

File format: .MP4

Title of data: Video of Supported Forward Sway

Description of data: De-identified video of a participant performing the supported forward sway activity.

File name: Additional file 3

File format: MP4

Title of data: Video of Supported Backward Sway

Description of data: De-identified video of a participant performing the supported backward sway activity.

File name: Additional file 4

File format: MP4

Title of data: Video of Perturbed Forward Sway

Description of data: De-identified video of a participant performing the perturbed forward sway activity.

File name: Additional file 5

File format: MP4

Title of data: Video of Perturbed Backward Sway

Description of data: De-identified video of a participant performing the perturbed backward sway activity.

File name: Additional file 6

File format: .DOCX

Title of data: Compilation of All Participants' BRs

Description of data: All original and normalized BRs for each participant, where the left column is the original BR and the right column is the normalized BR.

File name: Additional file 7

File format: .DOCX

Title of data: Table of COP rmANOVA Post-hoc Tests

Description of data: Table including the p-values of the post-hoc test outcomes from the rmANOVA comparisons for each COP metric (RMS, 95% ellipse area, mean velocity, range).

File name: Additional file 8

File format: .DOCX

Title of data: IK Results Grouped by Sex

Description of data: Average IK plots for male and female participants in the same formatting as Fig. 5.

ABBREVIATIONS

COP: center of pressure

GRF: ground reaction force

AP: anteroposterior

LIP: linear inverted pendulum

COM: center of mass

BoS: base of support

MoS: margin of stability

XcoM: extrapolated center of mass

BR: balance region

RL: reinforcement learning

IK: inverse kinematics

VS: voluntary sway

SS: supported sway

SSF: supported sway forward

SSB: supported sway backward

PSF: perturbed sway forward

PSB: perturbed sway backward

RMS: root mean square

rmANOVA: repeated measures analysis of variance

BMI: body mass index

DECLARATIONS

Ethics approval and consent to participate

All procedures were approved by the Institutional Review Board at the New Jersey Institute of Technology (IRB#:2212027868) in accordance with the Declaration of Helsinki, and all participants provided written informed consent prior to participation.

Consent for publication

The use of de-identified images and videos for publication was included in the informed consent and obtained from all participants.

Availability of data and materials

The datasets used and/or analyzed during the current study are available from the corresponding author on reasonable request.

Competing interests

The authors declare that they have no competing interests.

Funding

The authors at NJIT gratefully acknowledge the financial support provided by the CDC's National Institute for Occupational Safety and Health for this research (Contract #: 75D30120P08812). Zhou is also partially supported by the National Science Foundation (NSF) under Grant GCR-2524089 and by the National Institute on Disability, Independent Living, and Rehabilitation Research (NIDILRR) under Grant 90REGE0025.

Authors' contributions

KA and XZ designed the experiments. KA, NR, and RJ recruited participants for the study and performed the experiments. KA developed the codes, analyzed the data, and wrote the main manuscript text. NR, RJ, and MD wrote parts of the introduction. CM, JD, and XZ supervised the work. All authors reviewed the manuscript.

Acknowledgements

We would like to thank Hans Elijah Hugo for his help in processing the inverse and body kinematics in OpenSim and Joshua Failla for his help with determining the COM velocity zero-crossings.

REFERENCES

1. Peterka RJ. Chapter 2 - Sensory integration for human balance control. In: Day BL, Lord SR, editors. Handbook of Clinical Neurology. 159: Elsevier; 2018. p. 27-42.

2. Winter DA. Human balance and posture control during standing and walking. Gait & Posture. 1995;3(4):193-214. https://doi.org/10.1016/0966-6362(96)82849-9

3. Winter DA, Patla AE, Frank JS. Assessment of balance control in humans. Med prog technol. 1990;16(1-2):31-51.

4. Prieto TE, Myklebust J, Raymond, Hoffmann, Lovett EG, Myklebust BM. Measures of postural steadiness: differences between healthy young and elderly adults. IEEE Transactions on Biomedical Engineering. 1996;43:956-66.

5. Mackey DC, Robinovitch SN. Mechanisms underlying age-related differences in ability to recover balance with the ankle strategy. Gait & Posture. 2006;23(1):59-68. https://doi.org/10.1016/j.gaitpost.2004.11.009

6. Liu K, Wang H, Xiao J, Taha Z. Analysis of human standing balance by largest Lyapunov exponent. Computational intelligence and neuroscience. 2015;2015(1):158478.

7. Shelton AD, McTaggart EM, Allen JL, Mercer VS, Crenshaw JR, Franz JR. Does the effect of walking balance perturbations generalize across contexts? Human Movement Science. 2024;93:103158. https://doi.org/10.1016/j.humov.2023.103158

8. Lanska DJ. The Romberg sign and early instruments for measuring postural sway. Semin Neurol. 2002;22(4):409-18. 10.1055/s-2002-36763

9. Jonsson E, Seiger Å, Hirschfeld H. One-leg stance in healthy young and elderly adults: a measure of postural steadiness? Clinical Biomechanics. 2004;19(7):688-94. https://doi.org/10.1016/j.clinbiomech.2004.04.002

10. Miranda N, Tiu TK. Berg Balance Testing. StatPearls Publishing, Treasure Island (FL); 2025.

11. Di Carlo S, Bravini E, Vercelli S, Massazza G, Ferriero G. The Mini-BESTest: a review of psychometric properties. Int J Rehabil Res. 2016;39(2):97-105. 10.1097/mrr.0000000000000153

12. Kinzey SJ, Armstrong CW. The Reliability of the Star-Excursion Test in Assessing Dynamic Balance. Journal of Orthopaedic & Sports Physical Therapy. 1998;27(5):356-60. 10.2519/jospt.1998.27.5.356

13. Shumway-Cook A, Brauer S, Woollacott M. Predicting the Probability for Falls in Community-Dwelling Older Adults Using the Timed Up & Go Test. Physical Therapy. 2000;80(9):896-903. 10.1093/ptj/80.9.896

14. Quijoux F, Nicolaï A, Chairi I, Bargiotas I, Ricard D, Yelnik A, et al. A review of center of pressure (COP) variables to quantify standing balance in elderly people: Algorithms and open-access code. Physiological Reports. 2021;9(22):e15067. https://doi.org/10.14814/phy2.15067

15. Juras G, Słomka K, Fredyk A, Sobota G, Bacik B. Evaluation of the limits of stability (LOS) balance test. Journal of Human Kinetics. 2008;19(2008):39-52.

16. Pickerill ML, Harter RA. Validity and reliability of limits-of-stability testing: a comparison of 2 postural stability evaluation devices. J Athl Train. 2011;46(6):600-6. 10.4085/1062-6050-46.6.600

17. Petró B, Papachatzopoulou A, Kiss RM. Devices and tasks involved in the objective assessment of standing dynamic balancing – A systematic literature review. PLoS One. 2017;12(9):e0185188. 10.1371/journal.pone.0185188

18. Hof AL, Gazendam MGJ, Sinke WE. The condition for dynamic stability. Journal of Biomechanics2005. p. 1-8. 10.1016/j.jbiomech.2004.03.025

19. Curtze C, Buurke TJW, McCrum C. Notes on the margin of stability. Journal of Biomechanics. 2024;166:112045. https://doi.org/10.1016/j.jbiomech.2024.112045

20. Mummolo C, Mangialardi L, Kim JH. Numerical Estimation of Balanced and Falling States for Constrained Legged Systems. Journal of Nonlinear Science. 2017;27:1291-323. 10.1007/s00332-016-9353-2

21. Akbas K, Mummolo C. A Computational Framework Towards the Tele-Rehabilitation of Balance Control Skills. Front Robot AI. 2021;8:648485. 10.3389/frobt.2021.648485

22. Akbas K, Mummolo C. A Computational Framework Towards the Tele-Rehabilitation of Balance Control Skills. Frontiers in Robotics and AI. 2021;8. 10.3389/frobt.2021.648485

23. Mummolo C, Akbas K, Carbone G. State-Space Characterization of Balance Capabilities in Biped Systems with Segmented Feet. Front Robot AI. 2021;8:613038. 10.3389/frobt.2021.613038

24. Mummolo C, Mangialardi L, Kim JH. Numerical Estimation of Balanced and Falling States for Constrained Legged Systems. Journal of Nonlinear Science: Springer US; 2017. p. 1291-323. 10.1007/s00332-016-9353-2

25. Peng WZ, Mummolo C, Song H, Kim JH. Whole-body balance stability regions for multi-level momentum and stepping strategies. Mechanism and Machine Theory. 2022;174. 10.1016/j.mechmachtheory.2022.104880

26. Akbaş K, Mummolo C, Zhou X. Characterization of Human Balance through a Reinforcement Learning-based Muscle Controller. PloS one. 2025;20(4):e0320211.

27. Kajita S, Kanehiro F, Kaneko K, Fujiwara K, Harada K, Yokoi K, et al., editors. Biped walking pattern generation by using preview control of zero-moment point. 2003 IEEE International Conference on Robotics and Automation (Cat No03CH37422); 2003 14-19 Sept. 2003. 10.1109/ROBOT.2003.1241826

28. Kajita S, Morisawa M, Miura K, Nakaoka S, Harada K, Kaneko K, et al., editors. Biped walking stabilization based on linear inverted pendulum tracking. 2010 IEEE/RSJ International Conference on Intelligent Robots and Systems; 2010 18-22 Oct. 2010. 10.1109/IROS.2010.5651082

29. Zhang R, Zhao M, Wang C-L, editors. Standing push recovery based on LIPM dynamics control for biped humanoid robot. 2018 IEEE International Conference on Robotics and Biomimetics (ROBIO); 2018: IEEE.

30. Hall JC, Roberts BW, Bahari H, Forero J, Rouhani H, Hebert JS, et al., editors. clinical utility of gait stability measures: Selection and preliminary evaluation of the margin of stability. Current Directions in Biomedical Engineering; 2022: De Gruyter.

31. Koolen FA. Balance control and locomotion planning for humanoid robots using nonlinear centroidal models: Massachusetts Institute of Technology; 2020.

32. Kasaei M, Lau N, Pereira A. Comparison Study of Well-Known Inverted Pendulum Models for Balance Recovery in Humanoid Robot. arXiv preprint arXiv:190601936. 2019.

33. Era P, Schroll M, Ytting H, Gause-Nilsson I, Heikkinen E, Steen B. Postural Balance and Its Sensory-Motor Correlates in 75-Year-Old Men and Women: A Cross-

National Comparative Study. The Journals of Gerontology: Series A. 1996;51A(2):M53-M63. 10.1093/gerona/51A.2.M53

34. Scaglioni-Solano P, Aragón-Vargas LF. Gait characteristics and sensory abilities of older adults are modulated by gender. Gait & Posture. 2015;42(1):54-9. https://doi.org/10.1016/j.gaitpost.2015.04.002

35. Nigg BM, G KET, Federolf P, Landry SC. Gender differences in lower extremity gait biomechanics during walking using an unstable shoe. Clinical Biomechanics. 2010;25(10):1047-52. https://doi.org/10.1016/j.clinbiomech.2010.07.010

36. Espinoza-Araneda J, Bravo-Carrasco V, Álvarez C, Marzuca-Nassr GN, Muñoz-Mendoza CL, Muñoz J, et al. Postural balance and gait parameters of independent older adults: A sex difference analysis. International journal of environmental research and public health. 2022;19(7):4064.

37. Nolan L, Grigorenko A, Thorstensson A. Balance control: sex and age differences in 9- to 16-year-olds. Developmental Medicine & Child Neurology. 2005;47(7):449-54. https://doi.org/10.1111/j.1469-8749.2005.tb01170.x

38. Holden S, Boreham C, Delahunt E. Sex Differences in Landing Biomechanics and Postural Stability During Adolescence: A Systematic Review with Meta-Analyses. Sports Medicine. 2016;46(2):241-53. 10.1007/s40279-015-0416-6

39. Schedler S, Kiss R, Muehlbauer T. Age and sex differences in human balance performance from 6-18 years of age: A systematic review and meta-analysis. PLOS ONE. 2019;14(4):e0214434. 10.1371/journal.pone.0214434

40. Lin D, Seol H, Nussbaum MA, Madigan ML. Reliability of COP-based postural sway measures and age-related differences. Gait & Posture. 2008;28(2):337-42. https://doi.org/10.1016/j.gaitpost.2008.01.005

41. Olchowik G, Czwalik A, Kowalczyk B. The Changes in Postural Stability of Women in Early Old Age. J Nutr Health Aging. 2020;24(7):739-44. 10.1007/s12603-020-1399-z

42. Osoba MY, Rao AK, Agrawal SK, Lalwani AK. Balance and gait in the elderly: A contemporary review. Laryngoscope Investigative Otolaryngology. 2019;4(1):143-53. https://doi.org/10.1002/lio2.252

43. Pijnappels M, Reeves ND, Maganaris CN, van Dieën JH. Tripping without falling; lower limb strength, a limitation for balance recovery and a target for training in the elderly. Journal of Electromyography and Kinesiology. 2008;18(2):188-96. https://doi.org/10.1016/j.jelekin.2007.06.004

44. Tashiro H, Hirosaki S, Sato Y, Ihira H, Toki M, Kozuka N. Concern about falling is related to threat-induced changes in emotions and postural control in older adults. Gait & Posture. 2025;115:1-6. https://doi.org/10.1016/j.gaitpost.2024.10.020

45. Luo H, Wang X, Fan M, Deng L, Jian C, Wei M, et al. The Effect of Visual Stimuli on Stability and Complexity of Postural Control. Frontiers in Neurology. 2018;9. 10.3389/fneur.2018.00048

46. Raffegeau TE, Fawver B, Young WR, Williams AM, Lohse KR, Fino PC. The direction of postural threat alters balance control when standing at virtual elevation. Experimental Brain Research. 2020;238(11):2653-63. 10.1007/s00221-020-05917-5

47. Adkin AL, Frank JS, Jog MS. Fear of falling and postural control in Parkinson's disease. Movement Disorders. 2003;18(5):496-502. https://doi.org/10.1002/mds.10396

48. Maki BE, Holliday PJ, Topper AK. Fear of Falling and Postural Performance in the Elderly. Journal of Gerontology. 1991;46(4):M123-M31. 10.1093/geronj/46.4.M123

49. Sturnieks DL, Delbaere K, Brodie MA, Lord SR. The influence of age, anxiety and concern about falling on postural sway when standing at an elevated level. Human Movement Science. 2016;49:206-15. https://doi.org/10.1016/j.humov.2016.06.014

50. Chen C-L, Lou S-Z, Wu H-W, Wu S-K, Yeung K-T, Su F-C. Effects of the type and direction of support surface perturbation on postural responses. Journal of NeuroEngineering and Rehabilitation. 2014;11(1):50. 10.1186/1743-0003-11-50

51. Hwang S, Tae K, Sohn R, Kim J, Son J, Kim Y. The Balance Recovery Mechanisms Against Unexpected Forward Perturbation. Annals of Biomedical Engineering. 2009;37(8):1629-37. 10.1007/s10439-009-9717-y

52. Graham DF, Carty CP, Lloyd DG, Barrett RS. Muscle contributions to the acceleration of the whole body centre of mass during recovery from forward loss of balance by stepping in young and older adults. PLOS ONE. 2017;12(10):e0185564. 10.1371/journal.pone.0185564

53. Adjei E, Nalam V, Lee H. Sex Differences in Human Ankle Stiffness During Standing Balance. Frontiers in Sports and Active Living. 2020;2. 10.3389/fspor.2020.570449

54. Ericksen H, Gribble PA. Sex Differences, Hormone Fluctuations, Ankle Stability, and Dynamic Postural Control. Journal of Athletic Training. 2012;47(2):143-8. 10.4085/1062-6050-47.2.143

55. Uhlrich SD, Falisse A, Kidziński Ł, Muccini J, Ko M, Chaudhari AS, et al. OpenCap: Human movement dynamics from smartphone videos. PLOS Computational Biology. 2023;19(10):e1011462. 10.1371/journal.pcbi.1011462

56. Cao Z, Hidalgo G, Simon T, Wei SE, Sheikh Y. OpenPose: Realtime Multi-Person 2D Pose Estimation Using Part Affinity Fields. IEEE Transactions on Pattern

Analysis and Machine Intelligence. 2021;43(1):172-86. 10.1109/TPAMI.2019.2929257

57. Dyer PS, Bamberg SJM, editors. Instrumented insole vs. force plate: A comparison of center of plantar pressure. 2011 Annual International Conference of the IEEE Engineering in Medicine and Biology Society; 2011 30 Aug.-3 Sept. 2011. 10.1109/IEMBS.2011.6091678

58. Goetschius J, Feger MA, Hertel J, Hart JM. Validating Center-of-Pressure Balance Measurements Using the MatScan® Pressure Mat. Journal of Sport Rehabilitation. 2018;27(1). 10.1123/jsr.2017-0152

59. Al Borno M, O'Day J, Ibarra V, Dunne J, Seth A, Habib A, et al. OpenSense: An open-source toolbox for inertial-measurement-unit-based measurement of lower extremity kinematics over long durations. Journal of NeuroEngineering and Rehabilitation. 2022;19(1):22. 10.1186/s12984-022-01001-x

60. Tohfafarosh M, Ratnakumar N, Zurzolo L, Adamovich S, Zhou X. Interactive Gait Rehabilitation Through Gamified Real-Time Biofeedback and Adaptive Hip Exoskeleton Assistance: A Preliminary Evaluation. RehabWeek 2025 - International Conference on Rehabilitation Robotics (ICORR); May 12-16; Chicago, IL, USA2025.

61. Leardini A, Biagi F, Merlo A, Belvedere C, Benedetti MG. Multi-segment trunk kinematics during locomotion and elementary exercises. Clinical Biomechanics. 2011;26(6):562-71. 10.1016/j.clinbiomech.2011.01.015

62. Leardini A, Sawacha Z, Paolini G, Ingrosso S, Nativo R, Benedetti MG. A new anatomically based protocol for gait analysis in children. Gait & Posture. 2007;26(4):560-71. https://doi.org/10.1016/j.gaitpost.2006.12.018

63. Hamner SR, Seth A, Delp SL. Muscle contributions to propulsion and support during running. Journal of Biomechanics. 2010;43(14):2709-16. https://doi.org/10.1016/j.jbiomech.2010.06.025

64. Edelsbrunner H, Kirkpatrick D, Seidel R. On the shape of a set of points in the plane. IEEE Transactions on Information Theory. 1983;29(4):551-9. 10.1109/TIT.1983.1056714

65. Koen J. alphashape: A Python implementation of alpha shapes. 2025.